Analysis of Physical Conditions in Herbig-Haro Objects

Author: Maria Balaguer Prat.
*Facultat de Física, Universitat de Barcelona, Diagonal 645, 08028 Barcelona, Spain.**

Advisor: María Rosario Isabel López Hermoso

Abstract: The aim of this work is to search optical spectra of Herbig-Haro objects in Taurus star-forming region and analyse it to make a diagnosis on their physical conditions. We study the degree of excitation, tracers of electron density, electron temperature and degree of ionization that are properties which are studied by the analysis on the forbidden emission lines. From a total of 57 catalogued objects, the lines of a sample of 30 knots are presented. It is obtained a range on electron temperature from $0.9 \times 10^4 K$ and $> 1.5 \times 10^4 K$, an average electron density of $2.5 \times 10^3 cm^{-3}$ and a minimum electron excitation of 15%.

Key words: *Herbig-Haro Object* (HH), *Taurus region*, *nebular diagnosis*, *optical spectra.*

I. INTRODUCTION

The study of the star formation regions provides wide information on the primarily period of the star's evolution.

A star is formed within a molecular cloud due to the gravitational collapse of dense cores. Due to the preservation of angular momentum and the gravitational pull between the particles into the nebulous, the surrounding material accumulates in an accretion disk around the protostar. Material from the disk is added via accretion at the star mass, it loses energy by viscosity, and falls into the star. The star ejects part of this additional material at high speeds. The accretion disk acts as a collimator, imposing a privileged direction that the ejected material will follow. These collimated high speed ejections of matter (of the order of hundreds of km/s) are the outflows. The particular ones that are manifested in the optical and infrared spectrum are called jets.

The ejected matter will interact with the surrounding material producing shocks, thus forming dense and excited aligned knots until a bow shock. This phenomena is called Herbig Haro (HH). The gas heated in the collisions is cooled via radiation, emitting permitted or forbidden lines (following electrical dipole selection rules). The forbidden lines are typical of the jets as they are characterised by low densities.

More than sixty years ago, George Herbig and Guillermo Haro independly detected the first object with these characteristics in the Orion region. From then, more than four hundred HH have been identified in different regions and catalogued [1]. In this work we focus on the study of the HH objects in the Taurus region.

The main objective of this work is to determine the physical properties of the HH in Taurus via the spectral analysis of the optic emission lines.

The work is divided in two parts: In the first one, we present the data acquisition of the optical line fluxes on Hβ, [O III] λ 5007Å, [OI] λ 6300, 6364Å, [NII] λ 6548, 6583Å, Hα and [SII] λ 6716, 6731Å. In the second part, the tracer ratios are analysed to obtain the physical characteristics of the objects.

Other similar study has been done in the Orion region by A. Algarra [2]. The obtained results are compared in the discussion section.

II. DATA COLLECTION

The data analysed in this work describe the HH objects located in the Taurus region, the nearest star-forming molecular cloud (140pc) which has specific properties because of its young age (1Myr) [3]. These data include fluxes from the lines mentioned in the previous section in which we are interested. The followed steps for the data collection has been the selection of objects via Reipurth catalogue obtained with the VIZIER database [4] by its coordinates and the search for optical spectra database. This step has been the most complex one. From more than 57 catalogued HH objects and more than 300 published papers, only a sample of 30 knots has numerical published accessible spectra information that we present in Table III. Our starting point regarding line fluxes has been the paper by A. C. Raga et al. "A Compilation of Optical Spectrophotometry of HH Objects and its Tentative Interpretation" [5]. Thus, the main part of the information in this section has been taken from papers from 1996 until 2019.

III. RESULTS

In this section, an analysis of the data presented in Table III (see Appendix) is carried out. Next figures represent the tracers of the studied physical conditions. The analysis of the spectra excitation characteristics of the studied objects has been based in the criteria showed in [5]. The analysis of the electron temperature, electronic excitation and electronic density are based on radiative transport equations (see example at [6]).

*Electronic address: mbalagpr7@alumnes.ub.edu

Due to the different sources of information, it has been complex to establish a common criteria to present and analyse the data. It has to be mentioned that the data from [7] do not correspond to the HH objects alone, since it is a study of young embedded stars. However, we ratify the use of this information due to the fact that the knots it presents are close to its star: HH 360A is a compact nebula close to IRAS 0416+2610 (360A and 360B are the names we have chosen for two knots found by Kenyon et al. [8]), HH 156 is a small bipolar jet near Coku Tau 1 [9], HH 31 IRS 2 is the name of a likely energy source (HH 31) found by Cohen & Schwartz [10], HH 414/413 is a small bipolar jet coinciding with its source IRAS 04264+2433 [11] and HH 408 is a bipolar flow consisting in two short jets and other bow shock associated with the T Tauri star Haro 6-33 (IRAS 04385+2550). It is important to stress that the information used emains the jet part that is closest to the star. Thus, we can consider it. The case of HH 30 is an example, whose data comes from both two different papers and allows us to compare the differences between one [7] (regarding the star) and the other [5].

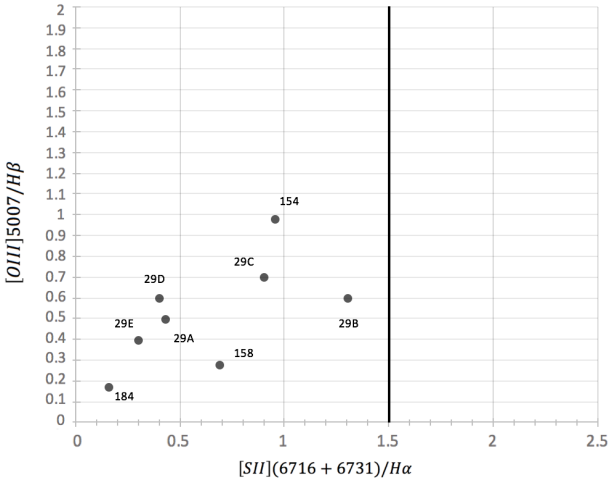

FIG. 1: Spectra excitation. The line limits the high excitation zone (left). Only the objects with [OIII] data are showed. All of them have high excitation spectra.

In Figure 1 we present the studied knots according to the excitation degree of their spectrum (high, intermediate or low), using the criteria given in [5]:

i) "high excitation spectra", with [O III] 5007/Hβ > 0.1 and [S II] (6716+6731)/H$\alpha \leq$ 1.5,

ii) "intermediate excitation spectra", with [O III] 5007/H$\beta \leq$ 0.1 and [S II] (6716+6731)/H$\alpha \leq$ 1.5,

iii) "low excitation spectra", with [O III] 5007/H$\beta \leq$ 0.1 and [S II] (6716+6731)/Hα > 1.5.

In Figure 2 a diagram of the behaviour of the tracers of electron density versus excitation is showed. From this representation, electron density can be obtained.

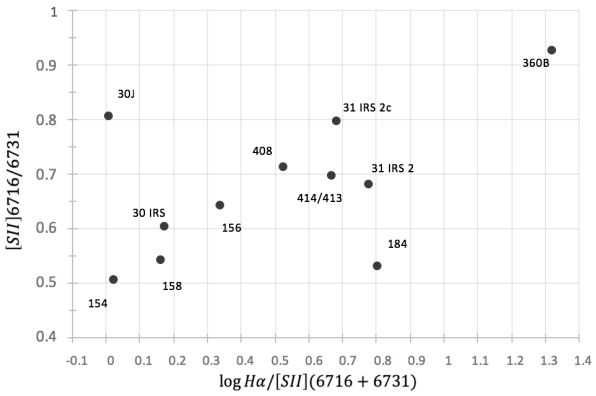

FIG. 2: Density tracer ([SII]6716/6731) versus excitation.

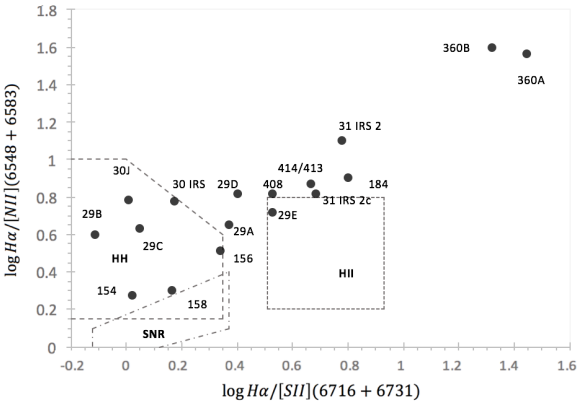

FIG. 3: Regions with HH, SNR (Supernova Remnants), and HII regions characteristics are delimited with dashed lines.

In Figure 3 we represent tracers of excitation: Hα/[SII] (6716+6731) and Hα/[NII] (6548+6583) these tracers give us information on the mechanism of emission lines. The represented regions are outlined using figure from [12] which is used in other articles as [13].

It is remarkable that, both in Figure 2 and Figure 3, the 360B and 360A objects appear considerably distant of the others. Thus, it might be because they are strongly perturbed by their surrounding sources.

Figures 4 and 5 show histograms regarding the decimal logarithm of the tracer of electron temperature ([O I]/[S II] (6300+6364/6716+6731)) and the decimal logarithm of the tracer of degree of ionization ([N II]/[O I] (6584/6300)).

IV. DISCUSSION

In this section we discuss the studied characteristics of the knots.

The criteria used for the study has provided the general characteristics of the discussed HH objects.

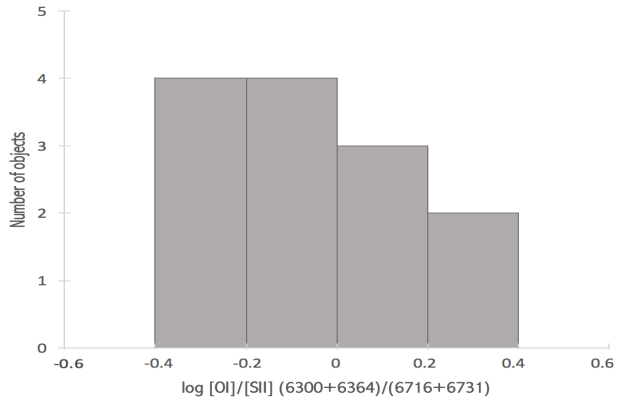

FIG. 4: Histogram of the distribution on the logarithm of the tracer of electron temperature [OI/SII].

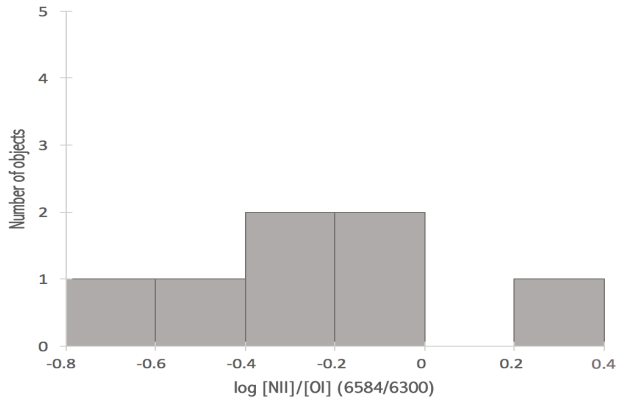

FIG. 5: Histogram of the distribution on the logarithm of the tracer of ionization degree. The range of ionization of our studied objects is from 15% until more than 60% (limit on $x = 0.4$).

A. Physical Conditions

It is worth to highlight that the majority of the HH objects that have been studied are the ones with more excited spectra defined as "high" or "intermediate excitation spectra". In Figure 1 there are only presented the objects that have [OIII]5007 and the excitation of its spectrum has been fully analysed. However, we notice that, regarding [SII]/$H\alpha$, the rest of the objects will belong to the high excited and intermediate excited spectra. From the results we can extract the statistical values on the physical conditions of our sample (Table I).

In Table II, corresponding values of the magnitudes from the tracers showed in Table I are presented.

Comparing these sample results with the ones presented in A. Algarra work [2], it is remarkable that, in general, T_e of the Taurus jets is higher than in the Orion region jets. The sample of study of this work has a shorter range regarding electron excitation (χ_e) than in the Orion sample. Furthermore, the maximum value of the density tracer (n_e) is lower than in the Orion sample.

	$[OI]/[SII](T_e)$	$[NII]/[OI](\chi_e)$	$(6716/6731)(n_e)$
Average	0.98	0.67	0.68
Deviation	0.49	0.48	0.13
Minimum	0.44	0.25	0.51
Maximum	1.85	1.65	0.93

TABLE I: Statistical values obtained for the studied ratios. Tracers of electron temperature, ionization degree and electron density.

	$T_e(10^4K)$	$\chi_e(\%)$	$n_e(10^3cm^{-3})$
Average	-	-	2.5
Minimum	0.9	15	0.8
Maximum	> 1.5	> 60	11.0

TABLE II: Limit values obtained for each magnitude. The average value on electron density is showed.

V. CONCLUSIONS

- It is found that in the Taurus region high excitation HH objects represent the total of the HHs that has data.
- Due to the lack of information, we cannot determine whether the used set of spectra data, and, therefore, the set of HHs analysed, are representative of the kind of objects in Taurus region. This lack of numeric spectroscopic observations database implies the difficulty of performing a statistical study of the physical conditions of these objects.
- It is corroborated that the effects of irradiation affect on the emission spectra of some of the studied HH as in HH 360.
- The comparison with the Orion region shows that the sample used in this work has narrower ranges of χ_e and n_e and a smaller deviation. Regarding T_e, we obtained larger values.

VI. APPENDIX

In the last page, we present the table that contains the studied objects and their spectral line fluxes. The objects are ordered by right ascension. The coordinates of the HH are mostly from Reipurth catalog. However, those specific knots that were found in J1950 had been transformed to J2000 using [14].

Acknowledgments

I would like to thank my advisor, Rosario López, for her encouragement and patience, my colleagues for sharing this wonderful path, Enrique Herrero for being there since I decided to start the my degree studies, Joan Ferrando for his unconditional confidence and my family.

[1] B. Reipurth and S. Heathcote. 50 Years of Herbig-Haro Research. From discovery to HST. In B. Reipurth and C. Bertout, editors, *Herbig-Haro Flows and the Birth of Stars*, volume 182 of *IAU Symposium*, pages 3–18, 1997.

[2] A. Algarra Diagnosis of Physical Conditions in Herbig-Haro Ob jects. TFG, UB 2018.

[3] K. L. Luhman, P. R. Allen, C. Espaillat, L. Hartmann, and N. Calvet. The Disk Population of the Taurus Star-Forming Region., 186:111–174, Jan 2010.

[4] "Strasbourg Astronomical Data Center," [Online]. Available: http://vizier.u-strasbg.fr. [Accessed 2019].

[5] A. Raga, K.-H Böhm, and J. Cantó. A compilation of optical spectrophotometry of HH objects and its tentative inter- pretation. *Revista Mexicana de Astronomía y Astrofísica*, 32:161–174, Sep 1996.

[6] L. Podio, S. Medves, F. Bacciotti, J. Eisloffel, and T. Ray, Physical structure and dust reprocessing in a sample of HH jets. *A&A*, 506(2):779–788, 2009.

[7] S. J. Kenyon, D. I. Brown, C. A. Tout, and P. Berlind. Optical spectroscopy of embedded young stars in the taurus-auriga molecular cloud. *The Astronomical Journal*, 115(6):2491–2503, Jun 1998.

[8] B. A. Whitney, S. J. Kenyon, and M. Gomez. Near-infrared imaging polarimetry of embedded young stars in the taurus-auriga molecular cloud. *The Astrophysical Journal*, 485(2):703–734, Aug 1997.

[9] M. Cohen and L. V. Kuhi. Observational studies of pre-main-sequence evolution.*Astrophys. J., Suppl. Ser.*, 41:743–843, Dec 1979.

[10] M. Cohen and R. D. Schwartz. The exciting stars of Herbig-Haro objects. *Astrophys. J.*, 265:877–900, Feb 1983.

[11] D. Devine, B. Reipurth, J. Bally, and T. J. Balonek. A giant herbig-haro flow from haro 6-10. *The Astronomical Journal*, 117(6):2931–2940, Jun 1999.

[12] J. Cantó, in Investigating the Universe, Dordrecht: Reidel, F. Khan, 1981, p. 95.

[13] R. López, R. Estalella, G. Gómez, A. Riera, and C. Carrasco-González. The nature of HH 223 from long- slit spectroscopy. *A&A*, 498(3):761–769, May 2009.

[14] Green R. M. Spherical Astronomy, Cambridge University Press, 1985.

[15] P. M. Garnavich, A. Noriega-Crespo, and P. J. Green. Wide field imaging of the star forming region Lynds 1551. *Revista Mexicana de Astronomía y Astrofísica*, 24:99–107, Apr 1992.

[16] C. V. M. Fridlund, R. Liseau, and E. Gullbring. The physical structure of the Herbig Haro object HH 29. *A&A*, 330:327–335, Feb 1998.

TABLE III
FLUXES OF HH OBJECTS RELATIVE TO Hβ=100

HH	R.A.(J2000) (^{hms})	Decl.(J2000) (^{o} $'$ $''$)	[O III] λ 5007 Å	[O I] λ 6300 Å	[O I] λ 6364 Å	[N II] λ 6548 Å	[Hα] λ 6563 Å	[N II] λ 6583 Å	[S II] λ 6716 Å	[S II] λ 6731 Å
360B	04 04 42.9	+26 18 42					56.0	1.4	1.3	1.4
360A	04 04 43.0	+26 19 00					55.5	1.5	2.0	
156	04 18 51.5	+28 20 28		71.5	23.0		110.5	33.5	20.0	31.0
158	04 27 04.7	+26 06 16	28	114			378	188	92	169
31	04 27 57.3	+26 19 18								
31 IRS 2c							86.0	13.0	8.0	10.0
31 IRS 2							95.0	7.5	6.5	9.0
184	04 29 23.7	+24 33 01	17	369			2074	259	115	215
414/413	04 29 30.3	+24 39 54		23.0	7.0		78.5	10.5	7.0	10.0
256-GH1	04 30 53.2	+17 59 07							263	
258-GH2	04 30 58.0	+18 03 35							76	
258-GH3	04 30 58.6	+18 04 02							39	
258-GH4	04 31 01.2	+18 04 01							62	
258-GH5	04 31 01.2	+18 03 38							158	
258-GH6	04 31 01.9	+18 02 55							118	
258-GH7	04 31 04.1	+18 03 49							225	
258-GH8	04 31 05.9	+18 03 31							103	
259-SH229	04 31 14.1	+18 04 02							50	
29	04 31 27.1	+18 06 24							33	
29A			50	35		22			43	
29B			60	70		25			130	
29C			70	50		23			90	
29D			60	62		15			40	
29E			40	20		19			30	
29F				10					10	
261-SH219/220	04 31 30.0	+18 06 53							9	
154	04 31 33.8	+18 08 02	98	1477			2500	1310	803	1578
30 J	04 31 37.6	+18 12 26		526			813	132	358	443
30 IRS				110.0	35.0		185.0	30.5	47.0	77.5
262-GH9	04 31 58.9	+18 12 07							65	
262-GH10W	04 32 00.1	+18 11 34							85	
262-GH10E	04 32 01.1	+18 11 24							102	
408	04 41 38.9	+25 56 26					20.0	3.0	2.5	3.5

TABLE III: The data for 360B, 360A (also known as 04016+2610), 156, 31 IRS 2c (also known as 04248+2612), 31 IRS 2, 414/413, 30 IRS and 408 is from [7]. HH 158, 184, 154 and 30 are from [5]. Source of HH 256, 258, 259 and 262 is [15]. The data of the HH 29 knots is from [16].
The [OI], [NII] and [SII] fluxes of the HH 29, 256, 258, 259, 261 and 262 knots are relative to Hα = 100 due to the lack of Hβ normalized information.